Initial Conditions for Parabolic Calculation of Reacting Flows

Eugene F. Brown*
Virginia Polytechnic Institute and State University, Blacksburg, Virginia

and
R. Clayton Rogers†
NASA Langley Research Center, Hampton, Virginia

A parabolic combustion code called CHARNAL was run for a variety of measured and estimated inlet boundary conditions. A parametric study was carried out to determine what compromises in accuracy would occur if estimated inlet conditions were used and what values of the dissipation length scale would give the best results. The conclusions were that a dissipation length scale of 0.03 gave the best results in all cases, regardless of the type of inlet conditions used. Both subsonic and supersonic flow were examined and the effect of finite rate vs equilibrium chemistry calculations was briefly considered. No significant compromises in accuracy were found when estimated inlet boundary conditions were used.

Nomenclature

d_j = fuel jet diameter
D = outer stream diameter, see Fig. 1
EPS = mean error, see Eq. (2)
EPS_j = profile error, see Eq. (1)
k = turbulent kinetic energy
ℓ_ϵ = dissipation length scale
M = Mach number
N = total number of values in a measured data set
p = pressure
p_i = predicted value of a parameter (temperature, concentration, etc.) at each measurement location
P_i = measured value of a parameter (temperature, concentration, etc.) in a data set
r = radial position
R = effective radius of the fuel jet
T = temperature
u = local velocity
U = centerline velocity
δ = shear layer thickness
δ_i^* = incompressible displacement thickness
ϵ = kinematic eddy viscosity

Introduction

ACCURATE prediction of chemically reacting flows requires accurate specification of the boundary conditions. Several excellent papers are available in which the sensitivity of both reacting and nonreacting calculations to the specification of the velocity and turbulence kinetic energy at the inlet is examined. Singled out in these papers for particular attention are the conditions at the combustor inlet. Sturgess et al.,[1] for example, considers the effect of various estimates of the inlet velocity profile on the downstream predictions of turbulence kinetic energy. In a particularly thorough consideration of this problem, Fabris et al.[2] recommend that estimates of the inlet conditions be avoided and suggest that experimental measurements of the inlet conditions be used if at all possible.

Received May 17, 1985; presented as Paper 85-1251 at the AIAA/SAE/ASME 21st Joint Propulsion Conference, Monterey, CA, July 8-10, 1985; revision received Nov. 21, 1985.

*Associate Professor. Associate Fellow AIAA.
†Aerospace Engineer. Member AIAA.

In addition to the velocity and turbulence kinetic energy, the use of the so-called k-ϵ turbulence model requires the specification of an additional quantity—the value of the turbulence dissipation. The Prandtl-Kolmogorov hypothesis enables the turbulence dissipation to be specified in terms of the inlet turbulence kinetic energy; however, specification is required of yet another empirical parameter—the value of the dissipation length scale.

Unlike the "constants" in the k-ϵ model, the dissipation length scale is often looked upon as an adjustable parameter selected in order to obtain the best fit of the calculations to whatever experimental data are available. An example of such an application is the CHARNAL code[3] written for NASA Langley. The code makes use of a parabolized Navier-Stokes calculation and contains both equilibrium and finite rate chemistry models.

This work seeks to address several questions with regard to the effect of the inlet boundary conditions employed in the CHANAL program:

1) What is the "best" value of the dissipation length scale?
2) How does this value depend upon the inlet velocity and turbulence kinetic energy profiles?
3) Are different values required for subsonic and supersonic flow?
4) What are the likely compromises in accuracy that will result from using estimated inlet conditions?

In order to answer these questions, a parametric study was conducted in which three test cases were run: an equilibrium chemistry calculation for a subsonic burner described by Antcliff et al.,[4] an equilibrium chemistry calculation for a supersonic burner made by Evans et al.,[5] and a finite rate chemistry calculation for the Evans burner. In Refs. 4 and 5, calculations using the CHARNAL code were described; however, no systematic study of the proper choice of the dissipation length scale or of the effect of different inlet boundary conditions was carried out.

Accuracy Criterion

In order to determine the "best" value of the dissipation length scale and to determine the consequences of using estimated inlet conditions, a quantitative measure of the accuracy of the CHARNAL calculations was required. For this purpose a profile error EPS_j was defined,

$$EPS_j = \left[\frac{1}{N}\sum_1^N (P_i - p_i)^2\right]^{1/2} \Big/ \frac{1}{N}\sum_1^N p_i \qquad (1)$$

where N is the number of experimental data points, P_i the measured parameter (temperature, concentration, etc.), and p_i the predicted value at each point a measurement is made. The profile error can be interpreted as the root-mean-square (rms) deviation of the calculations from the experimental data divided by the mean of the experimental data. From the profile error, a mean error was computed by averaging each of the profile errors. The mean error EPS is defined by

$$\text{EPS}=\frac{1}{M}\sum_{1}^{M}\text{EPS}_j \tag{2}$$

where M is the total number radial and/or axial traverses carried out in the experiment.

Calculations

Calculations of the axisymetric co-flowing fuel and air jet flowfield were made with the CHARNAL computer code.[3] This code solves the parabolized Navier-Stokes equations for the turbulent mixing of hydrogen and air with chemical reaction. The equations are solved in stream-function coordinates to obtain radial profiles of the flow properties at each axial station with a marching finite difference numerical integration procedure.

For the present calculations, 39 points were used in the radial profiles, giving 38 stream tubes. The calculations were begun with points in the initial profiles selected to adequately define the fuel jet flow and the shear layer between the fuel and air flows. As the two jets mix and burn, causing spreading of the streamlines, some details of the profiles may be lost, since the radial positions draw farther apart. Because the code has been used for numerous calculations of this type (e.g., Ref. 5), this feature of the solution is not considered to be detrimental so long as care is taken in selecting the initial profile positions.

Subsonic Burner

This burner, described in Antcliff et al,[4] consists of a hydrogen fuel jet surrounded by a coaxial airstream. The nominal velocity of the hydrogen jet was 100 m/s and that of the air jet 15.5 m/s. Both streams were at ambient temperature and pressure. Additional details of the experiment are given in Fig. 1 and Table 1.

In order to investigate the sensitivity of the "best" dissipation length scale to different choices for the inlet velocity and turbulence kinetic energy profiles, three cases (A-C) of inlet conditions were considered. Case A consisted of using the measured profiles of velocity and turbulence kinetic energy. The measured data were obtained with a hot-wire anemometer.[4] Case B consisted of using the measured data for the velocity profile, but estimated the turbulence kinetic energy profile using the method of Fabris et al.[2] This method used the equation,[5]

$$k=3.33\,\epsilon\frac{du}{dy}=3.33U\delta_i^*\frac{\epsilon}{U\delta_i^*}\frac{du}{dy}$$

where U is the centerline velocity, δ_i^* the incompressible displacement thickness, and ϵ the kinematic eddy viscosity obtained from Maise and McDonald.[6] The value of the velocity gradient du/dy was obtained from a least squares curve fit of the measured velocity data. The following equations were used to fit the measured velocity profiles for the fuel jet

$$u/U=a[1-(r/R)]^b$$

and for the air jet

$$u/U=a(r/\delta)^b$$

where R is the effective radius of the fuel jet and δ the shear layer thickness of the air jet. These values were obtained from experimental data. The value R corresponded to the radius where the measured velocity was a minimum. The value of δ was taken as the radial distance from the minimum velocity point to the point where the velocity in the air jet reached 99% of its freestream value. For this case, the value of R was 2.56 mm and of δ was 1.00 mm. Curve fitting the fuel jet velocity profile produced values of a and b of 1.26 and 0.51, respectively. For the air jet, the corresponding values of a and b were 1.14 and 0.41, respectively. From the values of $a,b,R,$ and δ the value of δ_i^* can be calculated. The value of δ_i^* was 0.422 mm for the fuel jet and 0.191 mm for the air jet. For the determination of ϵ (actually $\epsilon/U\delta_i^*$), the curve labeled $M=0$ in Fig. 9 of Maise and McDonald[6] was used. The value of U for the fuel and air jets was adjusted until the computed and measured mass flow rates matched, which required a value of U of 135 m/s for the fuel jet and 18.4 m/s for the air jet.

Case C consisted of using both estimated velocity profiles and estimated turbulence kinetic energy profiles. For the velocity profiles, the above equations were again used; however, the values of a and b were obtained from the so-called one-seventh root law rather than a curve fit. Accordingly, the values of a and b used were 1.0 and 0.143, respectively. The value of R was the actual inner radius of the fuel tube (2.33 mm). The value used for ϵ was the estimated boundary-layer thickness. Fabris et al.[2] recommend using a value of 0.10 of the jet radius. The outer radius of the annular air tube was used for this radius, which resulted in a value of ϵ of 1.27 mm. Values of δ_i^* were calculated to be 0.278 mm for the fuel jet and 0.159 mm for the air jet. The turbulence kinetic energy was estimated from the resulting velocity profile in exactly the same way as case B. Matching the experimentally measured mass flow rates required a value of U of 139 m/s for the fuel jet and 18.4 m/s for the air jet.

Since measurements of the velocity profiles were made slightly downstream of the fuel tube exit, mixing between the fuel and air jets occurred. Therefore, it was necessary to approximate the concentration profiles for those cases in which the measured velocity profiles were used (cases A and B). For this purpose, the fuel jet was assumed to be composed entirely of fuel at radii less than the inner radius of the fuel tube and the air jet was assumed to be composed entirely of air at radii greater than the outer radius of the fuel tube. In the region between the inner and outer radii of the fuel tube, the concentrations of fuel and air were assumed to decline linearly to zero on the outer and inner radii, respectively. For case C, the

Table 1 Parameters of subsonic burner

Parameter	Hydrogen jet	Freestream
Mach number M	0.14	0.04
Temperature T, K	300	300
Velocity u, m/s	100	15.5
Pressure p MPa	0.1	0.1
Mass fraction		
a_{H_2}	0.223	0
a_{O_2}	0	0.232
a_{N_2}	0.776	0.768
a_{H_2O}	0	0

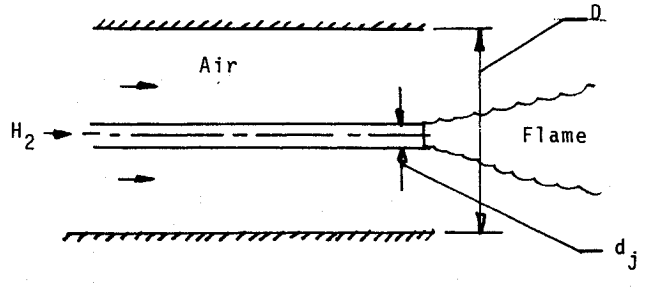

Fig. 1 Subsonic burner (from Ref. 4): $D=0.0254$ m; $d_j=0.0045$ m (inner) and the injector lip thickness = 0.00051 m.

Table 2 Subsonic initial conditions

Quantity	Case A		Case B		Case C	
	H_2	Air	H_2	Air	H_2	Air
R, mm	2.56	—	2.56	—	2.33	—
δ, mm	—	1.00	—	1.00	—	1.27
a	—	—	1.26	1.14	1.00	1.00
b	—	—	0.51	0.41	0.143	0.143
δ_j^*, mm	0.422	0.191	0.422	0.191	0.278	0.159
U, m/s	—	—	135	18.4	139	18.4

calculations were begun right at the fuel tube exit and, in addition, the fuel tube was assumed to be infinitesimally thin. Therefore, for case C calculations, the fuel and air concentrations dropped immediately to zero at the fuel tube radius. The initial conditions of the three cases are summarized in Table 2.

The velocity and turbulence kinetic energy profiles used in the calculations are shown in Fig. 2. The velocity profiles for all of the initial conditions are quite similar and so are the turbulence kinetic energy profiles for cases A and C. The levels of turbulence kinetic energy for case B are considerably higher than for either case A or C, however. The reason for this difference is due to the values of b, the exponent in the velocity profiles, since the gradient of the velocity profile on which the turbulence kinetic energy depends is directly proportional to exponent b. Inspection of Table 2 reveals that the value of b of case B is considerably greater than that of case C. Consequently, the levels of turbulence kinetic energy should be higher for case B as indicated in Fig. 2.

The reason that b is higher for case B than for case C is because the effects of mixing cause a "slimming" of the measured velocity profiles. The estimated velocity profiles are calculated at the fuel tube exit and, therefore, do not contain the effects of mixing. The estimated velocity profiles are, therefore, "fuller." From the velocity profile equations, it is easily seen that fuller velocity profiles have smaller values of b and consequently lower values of the turbulence kinetic energy.

For both cases B and C, the estimated turbulence kinetic energy at the centerline rises sharply. This sharp rise is due to the recommendation of Fabris et al.[2] that the centerline turbulence kinetic energy be set equal to the maximum value obtained on the profile. This constraint is necessary in order to prevent the turbulence kinetic energy from going to zero at the centerline where the velocity gradient vanishes.

In Fig. 3, the measured and predicted temperature profiles at two axial stations, 5.4 and 21.6 fuel tube inner diameters downstream of the injection plane, are shown. The solid line represents the calculations made with the measured inlet conditions (case A) and the broken line represents the calculations with the dissipation length scale, ℓ_ϵ/d_j of 0.03. Two facts are immediately apparent: 1) the agreement of the predicted and measured temperatures is much better at the upstream station than at the downstream station and 2), the calculations made with the estimated inlet conditions are not greatly different than those obtained with the measured inlet conditions. The situation is quite different if a different value of the dissipation length scale is used. This is shown in Fig. 4 where the measured temperature profile is again compared with the calculated values; however, a value of the dissipation length scale of 0.09 was used for the case C calculations. The resulting deterioration of the results clearly establishes the importance of properly choosing the dissipation length scale in order insure adequate agreement with the experimental data.

Figure 5 indicates a way in which the best value of the dissipation length scale can be chosen. In this figure, the mean error in temperature is plotted as a function of the dissipation length scale for the three inlet boundary conditions. Cases A and C show a clear minimum (and thus the best agreement with the measured temperatures) at a value of the dissipation length scale of 0.03. Figure 6 is similar to Fig. 5 except that the

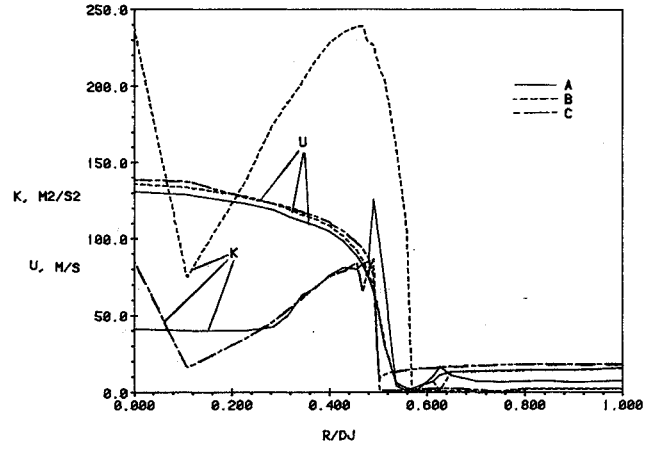

Fig. 2 Inlet boundary conditions (subsonic burner).

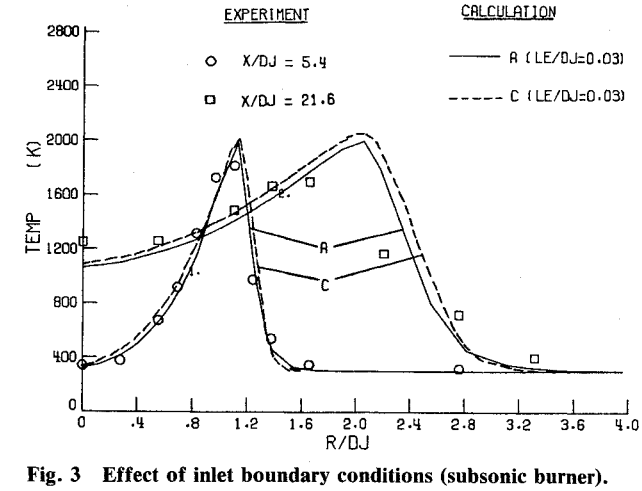

Fig. 3 Effect of inlet boundary conditions (subsonic burner).

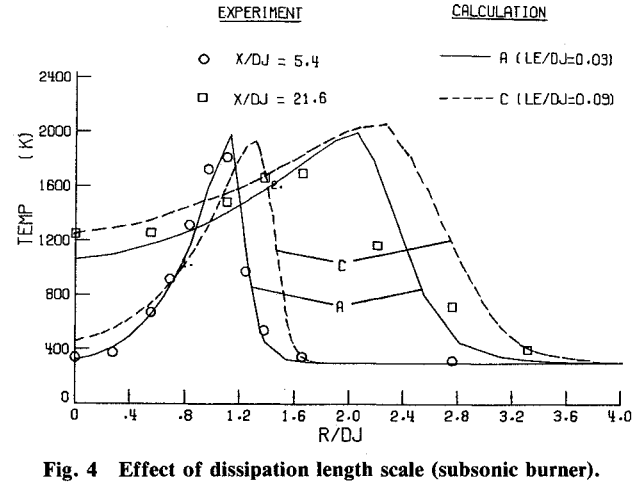

Fig. 4 Effect of dissipation length scale (subsonic burner).

average error in the nitrogen number density is plotted instead of the average error in temperature. Again for cases A and C, the best accuracy is found at a dissipation length scale of 0.03. An investigation of the profile error EPS_j also showed the best value of the dissipation length scale to be 0.03, except for the downstream radial profile where a value of 0.05 gave slightly better results. Accordingly, in Figs. 5 and 6, the region stretching from 0.03 to 0.05 on the abscissa is marked as the range in which the best value of the dissipation length scale lies. This value of the dissipation length scale is independent of whether measured or estimated boundary consitions are used. This result is because the error curves all have approximately the same shape and all reach their minimum values at approximately the same point. However, there is a difference in level. As might be expected, the lowest error is shown by the calculation using the measured inlet conditions (case A).

It is interesting to compare this range of dissipation length scales with the values found in the literature. In Launder and Spalding,[7] for example, one finds values of the mixing lengths divided by the "width of ½ jet" to be 0.075. Interpreting the "width of ½ jet" as the jet radius and assuming that the dissipation length scale is 0.548 times the mixing length (see Ref. 5), the value of the dissipation length scale is 0.021. This value is only slightly less than the range recommended above. Launder and Spalding also give a value of the mixing length obtained from Nikuradse's formula. Estimating the dissipation length scale from the mixing length in the manner just described gives a dissipation length scale of 0.04. This value is the midpoint of the range recommended above. Sturgess et al.[1] recommends a dissipation length scale of 0.03, which is also the value used by Antcliff et al.[4] This value is marked with an arrow in the preceding figures.

Until now, discussion of the results obtained with case B initial conditions has been avoided. There are two reasons for this: 1) the levels of turbulence kinetic energy in case B were considerably greater than either case A or C and 2) the values of the dissipation length scale required to give best agreement with the measured temperatures and nitrogen number densities (see Figs. 5 and 6) seem to be considerably greater than the values necessary for either case A or C and considerably greater than the values found in the literature. From this observation, it can be concluded that using measured values for the velocity profile and estimated values for the turbulence kinetic energy might not be advisable.

Supersonic Burner

Figure 7 and Table 3 describe the supersonic burner tested by Evans et al.,[5] which consists of a hydrogen fuel jet surrounded by an annular air jet; however, unlike the previous case, the jet velocities are supersonic. In these experiments, measurements of the total pressure in the jet and the species concentrations were made. There were no measurements made of the turbulence kinetic energy. Accordingly, it was impossible to carry out case A calculations. In the first calculations described below, the equilibrium chemistry option was used.

For case B calculations, the velocity profiles obtained from the measured pitot pressures were fit using the previously given velocity profile equations. The values of R and δ were selected as before. The resulting value of R was 4.29 mm and δ 2.48 mm. Curve fitting the fuel jet velocity profile produced a value of 1.10 for a and of 0.217 for b. Curve fitting the air jet

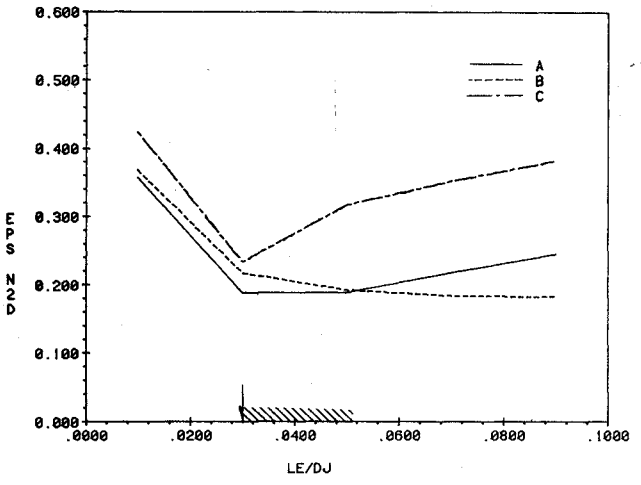

Fig. 6 Variation of nitrogen number density error with dissipation length scale (subsonic burner).

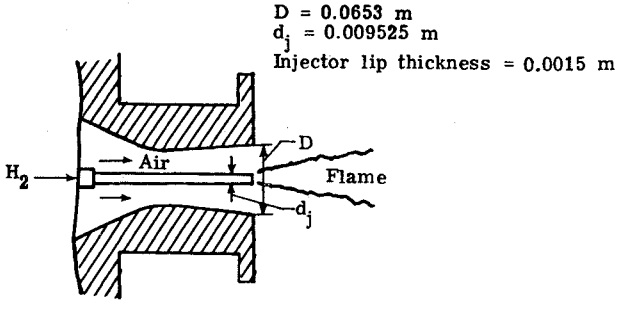

Fig. 7 Large-scale supersonic burner (from Ref. 5): $D = 0.0653$ m; $d_j = 0.009525$ m and the injector lip thickness = 0.0015 m.

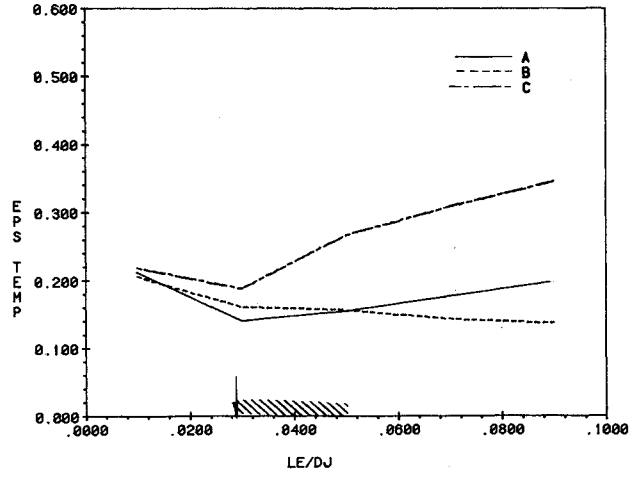

Fig. 5 Variation of static temperature error with dissipation length scale (subsonic burner).

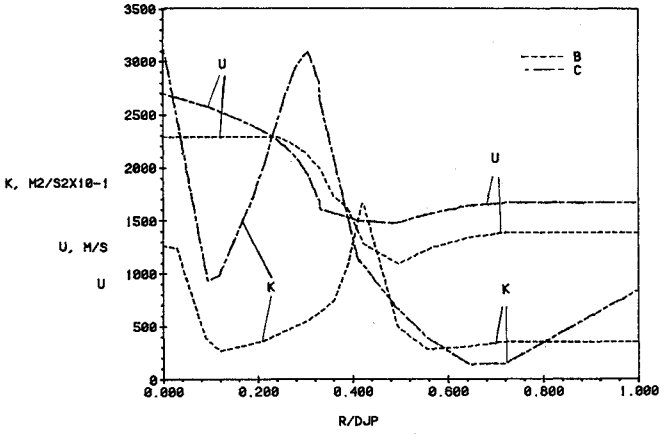

Fig. 8 Inlet boundary conditions (supersonic burner).

velocity gave a value of 0.940 for a and of 0.276 for b. The value of δ_i^* for the fuel jet was 0.312 mm and for the air jet 0.694 mm. The value of the kinetic eddy viscosity was again obtained from Maise and McDonald[6]; however, since the flow was supersonic, the curve labeled $M=2$ (rather than $M=0$) was used. The centerline velocities of the fuel and air jets were adjusted to match the measured mass flow rates, which required a value of 2432 m/s for the fuel jet and 1510 m/s for the air jet.

For case C, the value for R of 3.26 mm was used, which corresponded to the actual inner radius of the fuel tube. For the air jet, the value of δ was estimated to be 0.10 of the outer radius of the air tube, which gave a value of δ of 3.27 mm. The corresponding values of δ_i^* were 0.408 mm for both the fuel jet and the air jet. Matching the measured mass flow rates required a value of U of 2700 m/s for the fuel jet and 1670 m/s for the air jet. The concentration profile used for the case B calculations was approximately a linear variation over the width of the base of the fuel tube. For case C, calculations, however, a step change in concentration at the inner radius of the fuel tube was used just as in the case of the subsonic burner. In addition, for case C the fuel tube was assumed to be infinitesimally thin. The initial conditions of the three cases used in these calculations are summarized in Table 4.

In Fig. 8, the inlet values of velocity and turbulence kinetic energy used in the calculations are plotted as a function of the radius divided by the outer diameter of the fuel tube. The maximum velocities in the estimated fuel and air jets are slightly higher than the measured values in order to match the measured values of the mass flow rates. Unlike the subsonic jet case, the turbulence kinetic energy is greater for case C than for case B. This difference is because, even though the value of b is less in case C than in case B (as before), its effect on the turbulent kinetic energy is over shadowed by the significantly larger values of U and δ_i^* for case C (unlike the subsonic case).

In Fig. 9, the total pressure is plotted as a function of radius. Just as in Fig. 8, the radius is nondimensionalized by the outer diameter of the fuel tube. Results at two axial stations are shown: 6.56 and 26.2 fuel tube outer diameters downstream of the fuel tube exit. The case B calculations are represented by the solid line and the case C calculations by the broken line. Both calculations were carried out with a dissipation length scale (based on the outer diameter of the fuel tube) of 0.03. Neither calculation matches the measured results very well. However, case C seems to do slightly better than case B, even though the total pressures in the air jet seem to be too high. (In fact, these higher values of the total pressure might have been anticipated from the higher air jet velocities which were shown in Fig. 8.) Figure 10 shows the effect of increasing the dissipation length scale from 0.03 to 0.09. Clearly, this produces less favorable results. Figure 11 confirms this observation. In Fig. 11, the mean error in total pressure is plotted as a function of dissipation length scale. As the dissipation length scale increases, the agreement with the experimental results deteriorates. In addition at a dissipation length scale of 0.03, the case C calculations are superior, as previously observed. The cross-hatched region corresponds to the range of dissipation length scales recommended in the previous section for subsonic flow. (The values are now in the range of 0.02-0.03, however, because of the nondimensionalization with the outer fuel jet diameter.) The best agreement with the measured total pressures occurs for dissipation length scales slightly less than these values. A consideration of the mean error in hydrogen concentration showed that case C calculations predicted the measurements best. However, in this case, the best dissipation length scale lies near a value of 0.05. Finally, a consideration of the mean error in water vapor concentration showed that the optimum dissipation length scale is approximately 0.03.

Table 3 Parameters of supersonic burner

Parameter	Hydrogen jet	Freestream
Mach number M	2.00	1.90
Temperature T, K	251	1495
Velocity u, m/s	2432	1510
Pressure p, MPa	0.1	0.1
Mass fraction		
a_{H_2}	1.000	0
a_{O_2}	0	0.241
a_{N_2}	0	0.478
a_{H_2O}	0	0.281

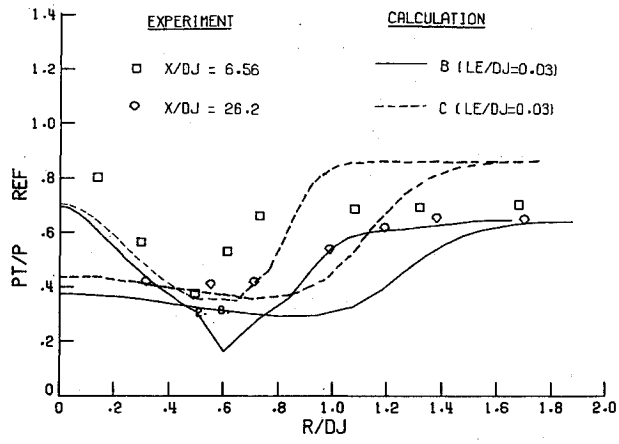

Fig. 9 Effect of inlet conditions (supersonic burner).

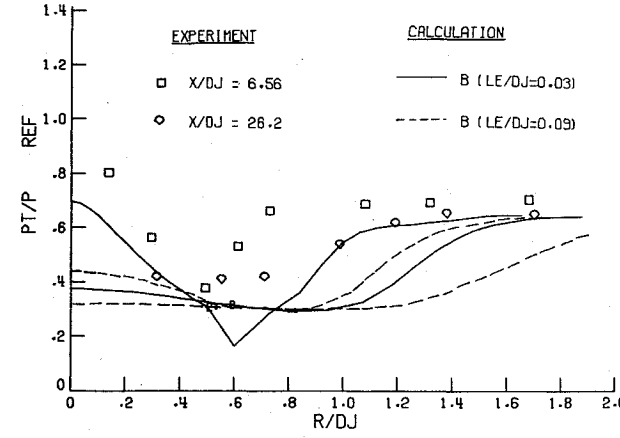

Fig. 10 Effect of dissipation length scale (supersonic burner).

Table 4 Supersonic inlet conditions

Quantity	Case B		Case C	
	H_2	Air	H_2	Air
R, mm	4.29	—	3.26	—
δ, mm	—	2.48	—	3.27
a	1.10	0.940	1.00	1.00
b	0.217	0.276	0.143	0.143
δ_i^*, mm	0.312	0.694	0.408	0.408
U, m/s	2432	1510	2700	1670

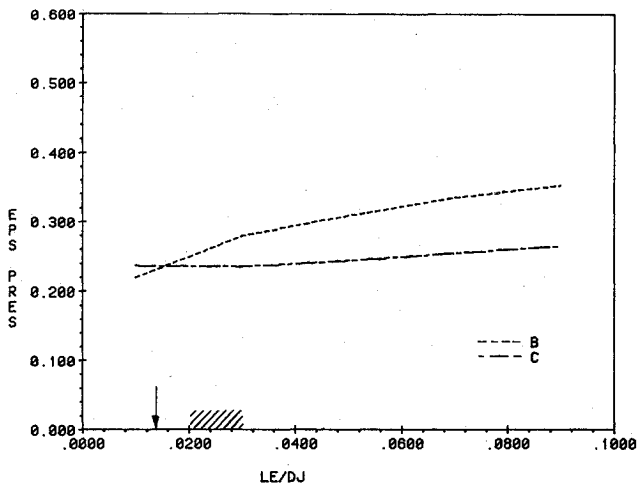

Fig. 11 Variation of total pressure error with dissipation length scale (supersonic burner).

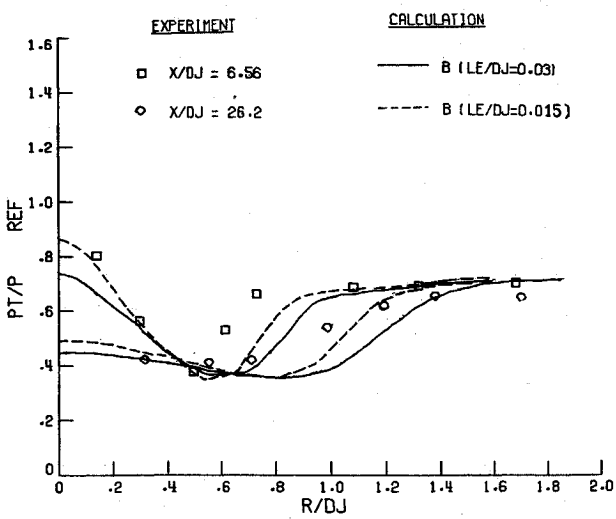

Fig. 12 Finite rate chemistry option (supersonic burner).

In Evans et al.,[5] a dissipation length scale of 10 times the lip thickness is recommended. Since the lip thickness is 0.0015 m, this gives a dissipation length scale of 0.015. The present study suggests that the optimum value is slightly higher, say 0.03. Putting the Evans recommended value on a consistent basis with the subsonic flow cases gives a value of dissipation length scale based on the inner fuel tube diameter of 0.04. Just as in the case of subsonic flow, the optimum dissipation length scale was independent of the inlet boundary conditions used.

The results obtained with the estimated velocity profile (case C) were, for all parameters, superior to the results obtained with the measured velocity profile. In part, this might be due to the way in which the velocity profiles were measured (see Ref. 5). However, it is interesting to note that this same effect was seen in the subsonic calculations where estimated velocity and kinetic energy profiles (case C) gave better results than the combination of an estimated kinetic energy profile and an experimental velocity profile (case B).

A significant improvement in the supersonic flow calculations was reported by Evans et al.[5] when finite rate calculations were used. To check the equilibrium chemistry option, two additional runs were made for the Evans' burner. The first was for a dissipation length scale of 0.03 and the second of 0.015. The kinetic model used in these calculations differs from that contained in the original CHARNAL code. It includes 32 reactions involving the 15 species H, O, H_2O, OH, O_2, H_2, N_2, N, NO, NO_2, HO_2, HNO_2, HNO_3, HNO, and H_2O_2. The reactions comprising the mechanism were obtained from published sources and verified by comparisons with more extensive mechanisms for the combustion of hydrogen in air. Because of the nature of the solution technique in the parabolic flow code with finite rate chemistry, it was necessary to prompt the chemical reaction by initializing the intermediate species (H, O, and OH) to small trace mass fractions of the order of 10^{-5}. Such a technique has been demonstrated successfully in other applications of the code.[5]

The results of the calculations for dissipation length scales of 0.03 and 0.015 and the case B inlet conditions are shown in Fig. 12. A significant improvement was obtained compared with the total pressures calculated with the equilibrium chemistry option (Fig. 9). The improvement is evident at both the near-field (6.56) and the far-field (26.2) locations. A calculation of the flow with a dissipation length scale of 0.015 results in still better agreement with the data at the 6.56 station, but somewhat poorer agreement at the 26.2 station.

Conclusions

For equilibrium chemistry, subsonic flow calculations, the results of this study indicate that the best value of the dissipation length scale (based on the inner diameter of the fuel tube) is 0.03. In addition, this value was also independent of the inlet conditions used. For equilibrium chemistry, supersonic flow calculations, the best value appears to be 0.04 (again based on the inner fuel tube diameter). Given the possibility of probe and sampling errors in the supersonic data, this small difference in the optimum value of the dissipation length scale should be ignored. Consequently, the value of 0.03 is recommended for both subsonic and supersonic flow. The use of finite rate chemistry appears to reduce the best value of the dissipation length scale to a value of less than 0.03. Insufficient runs have been made to determine a recommended value.

Acknowledgment

This work was carried out under the provisions of an Assignment Agreement (IPA) between NASA Langley and Virgina Polytechnic Institute and State University. We would like to thank Dr. H. L. Beach for making the necessary administrative arrangements to bring this about and Dr. G. B. Northam for providing valuable guidance during the course of this work.

References

[1]Sturgess, G. J., Syed, S. A., and McManus, K. R., "Importance of Inlet Boundary Conditions for Numerical Simulations of Combustor Flow," AIAA Paper 83-1263, June 1983.

[2]Fabris, G., Harsha, P. T., and Edelman, R. B., "Multiple-Scale Turbulence Modeling of Boundary Layer Flows for Scramjet Applications," NASA CR-3433, May 1981.

[3]Spalding, D. B., Launder, B. E., Morse, A. P., and Maples, G., "Combustion of Hydrogen-Air Jets in Local Chemical Equilbrium (A Guide to the CHARNAL Computer Program)," NASA CR-2407, June 1974.

[4]Antcliff, R. R., Jarrett, O. Jr., and Rogers, R. C., "CARS System for Turbulent Flame Measurement," AIAA Paper 84-1537, June 1984.

[5]Evans, J. S., Schexnayder, C. J. Jr., and Beach, H. L., "Application of a Two-Dimensional Parabolic Computer Program to Prediction of Turbulent Reaction Flows," NASA TP 1169, March 1978.

[6]Maise, G. and McDonald, H., "Mixing Length and Kinetic Eddy Viscosity in a Compressible Boundary Layer," *AIAA Journal*, Vol. 6, Jan. 1968, pp. 73-80.

[7]Launder, B. E. and Spalding, D. B., *Mathematical Models of Turbulence*, Academic Press, New York, 1972.